Vol 13 No 5, May 2004
1009-1963/2004/13(05)/0725-06

Chinese Physics

© 2004 Chin. Phys. Soc.
and IOP Publishing Ltd

Deposition behaviour of single Si adatom on $p(2\times2)$ Si(100) surface*

Huang Yan(黄 燕)[a)b)†] and Zhu Xiao-Yan(朱晓焱)[a)c)‡]

[a)] *Department of Physics, Soochow University, Suzhou* 215006, *China*
[b)] *National Laboratory for Infrared Physics, Shanghai Institute of Technical Physics, Chinese Academy of Sciences, Shanghai* 200083, *China*
[c)] *State Key Laboratory of Solid State Microstructures, Nanjing University, Nanjing* 210008, *China*

(Received 21 July 2003; revised manuscript received 26 December 2003)

The deposition of a single Si adatom on the $p(2\times2)$ reconstructed Si(100) surface has been simulated by an empirical tight-binding method. Using the perfect and defective Si surfaces as the deposition substrates, the deposition energies are mapped out around the research areas. From the calculated energy plots, the binding sites and several possible diffusion paths are achieved. The introduced defects will make the deposition behaviour different from that on the perfect surface.

Keywords: dimer vacancy, deposition, diffusion, empirical tight-binding
PACC: 6170E, 6610C, 7115F, 6810C

1. Introduction

The Si(100) surface has been extensively studied both theoretically and experimentally [1−9] since it is not only used for device fabrication but is also a relatively simple surface with complex reconstructions under various conditions of sample preparation. The behaviour of Si atoms on the surface plays an essential role in understanding the crystal growth. Because diffusion can reflect the nature of surface energy and interaction potentials, it is one of the essential parameters in controlling crystal growth. The development of scanning tunnelling microscopy (STM) technology [10] attracts much concentration to this research area. Many studies have focused on the binding and diffusing of atomic-scale Si ad-species on the Si(100) surface.[11−22]

However, it is well known that it is difficult to make a pure Si surface in practical sample preparation. There always exists a certain percentage of defects such as point defects, dimer vacancy (DV) etc.[1,7,23,24] Studies have shown that the surface properties are strongly influenced by defects.[25−27] Defective surface is supposed to be more suitable for growth than the perfect one since it can provide regions of low activation energy.

Okamoto *et al*[28] introduced the strain energy around a single-dimer vacancy (SDV) which makes their Monte Carlo simulation of the behaviour of buckled dimers on Si(100)(2×1) surface fit the experimental results well. The *ab initio* calculation finds that point defects are proper sites for the nucleation growth.[29] This type of defect lies underneath the surface. But both experiments [1] and theoretical studies [25] show that on the Si(100) surface the single atom defects are invisible. And from the STM images of Mo *et al*, the adatoms do not preferentially fill vacancies, which indicates the DV defects are not perfect traps.[30]

In this paper, the adsorption energy of an adatom on both perfect and defective $p(2\times2)$ Si surfaces is studied. For our model, we introduce single and double dimer vacancies into the perfect surface to form the defective one. By comparing the binding sites and the diffusion paths of the adatom on different surfaces, the influence of defects can be identified.

2. Method

In this work, the empirical tight-binding (ETB)

*Project supported by the Natural Science Foundation of Education Committee of Jiangsu Province, China (Grant No 00SJB140002).
†E-mail: hysherry@163.com
‡E-mail: zhuxy@suda.edu.cn

scheme [31–33] with steepest-descent (SD) method is used. We adopt the scheme of Ref.[34]. The Hellman–Feynman force on each atom in the system can be easily calculated by taking the derivative of the total energy with respect to its position. The whole method is testified to be efficient and accurate enough for various Si systems.[13,20,21,35,36]

The perfect supercell contains 160 Si atoms in which each layer is composed of 32 atoms, and each Si atom at the bottom layer is terminated with two H atoms to saturate the dangling bonds of the Si atoms. Two bottom Si layers and the additional H layer are fixed to prevent any spurious forces caused by the H atoms. A vacuum region of 0.6nm is used to simulate the bulk structure. The dimerization bonds are along the x direction [$\bar{1}$10], while the dimer rows on the surface are parallel to the y direction [110]. The periodic boundary conditions are applied to the x and y directions.

In all the calculations, the total energy is calculated only at Γ point of the first Brillouin zone of the unit cell, and the potential cutoff is 0.28nm to consider the nearest atom–atom interaction of Si only.

3. Results and discussion

In agreement with other calculations,[5,8,9] our study shows that both $c(4\times2)$ and $p(2\times2)$ reconstruction are energetically more favourable than other reconstructed phases such as asymmetric (2×1) structure (Table 1). In our work $p(2\times2)$ reconstruction is used. On the other hand, Hamers *et al*'s STM images [1] showed that the buckling is consistently larger near the missing dimer defect in each row and gradually decreases in going away from such defects. Their closer examination showed that a single defect can induce or stabilize the buckling of two or three atomic rows away. So the $p(2\times2)$ model can help to understand the influence of defects better.

Table 1. Total energy and dimer structure parameters of reconstructed Si(100) surfaces in different equilibrium states.

Structure	Total energy /(eV/dimer)	Bond length/nm	Δz/nm
$p(2\times1)$asym	0.128	0.244	0.065
$p(2\times2)$	0.012	0.243	0.076
$c(4\times2)$	0.0	0.243	0.076

3.1. Growth on perfect surface

The perfect Si(100) surface with $p(2\times2)$ reconstruction is studied first (Fig.1). This equilibrium structure is obtained from an ideal $p(2\times2)$ reconstruction relaxed by the SD method. The distance between the neighbouring dimer rows is 0.768nm, and in the same row, the distance between the dimers is 0.0384nm. The bond length of a dimer is 0.243nm with the asymmetry of 0.076nm, compared to 0.229 and 0.069nm from the pseudopotential calculations.[9] From the previous sp hybridization theory in the dangling bond of the distorted atoms, the electronic state changes to sp^2 (p_π) as the bond angle changes into 120° (90°). The bond angle of an up atom with adjacent atoms is 90.2°, close to 90°, enhancing the p_π character, whereas that of a down atom is 117.6°, close to 120°, enhancing sp^2. This surface structure agrees well with Jeong *et al*'s result.[32]

In order to simulate the growth process, we deposit an adatom on our sample surface at a series of sites within the range marked by a dashed rectangle in Fig.1 which form an equidistant grid with 0.096nm as the grid space in both x and y directions. The adatom is started at 0.28nm above the surface to have weak interaction with the surface atoms. Both x and y coordinates of the adatom are fixed, while the z coordinate is relaxed.

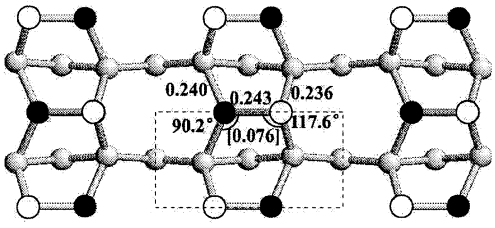


Fig.1. Top view of the fully relaxed $p(2\times2)$ Si(100) perfect surface (length unit is nm). Filled (open) circles represent down (up) atoms of the dimers. The grey circles indicate the substrate layer atoms, and the numbers in square brackets indicate the asymmetry of the dimers.

After all the grid points with the adatom are calculated, the deposition energy can be obtained. Although such an energy surface is a purely theoretical construct, we can extract a number of fundamental parameters from it. From the absolute minimum of the energy surface, we can identify the binding position of the adatom; and the saddle points of the energy surface give the activation energy or diffusion energy barriers for the migration of the adatom. We use M

and L to mark the absolute and local minimum points respectively. D labels the saddle points.

Our studies show that on the deposition energy of the perfect $p(2\times2)$ (Fig.2), the minimal point is near the lower dimer atom (not on the dimer bond), and beside the higher dimer atom is a local minimum, which is in conflict with the result of $p(2\times1)$ reconstruction. The *ab initio* calculation [11] shows that the binding site is near the D site. We attribute this difference to the different buckling structures. There are two possible diffusion paths: one is along the dimer row ($L_1 \rightarrow D_1 \rightarrow M_1$) with the energy barrier about 0.37eV; the other is a devious path ($M_2 \rightarrow D_2 \rightarrow M_1$) with an energy barrier about 0.59eV. Because the dimers are dynamically buckling [1] or flipping,[37] it is not ensured when the adatom diffuses along the dimer rows whether the nearest dimer atom is a higher or lower one. So the two paths can both be made use of for diffusion. But, if the path perpendicular to the dimer rows is chosen, the energy barrier will be up to 1.74eV. This higher energy barrier makes this kind of diffusion less possible. The high anisotropy is revealed by experimental [38] and theoretical [39] studies. In our study, the adatom cannot get onto the middle of the dimer which is a local minimum point of the $p(2\times1)$ surface [11] in *ab initio* calculation. In other words, the middle point of the dimer is a low point in the $p(2\times1)$ model, while it is a much higher point in the $p(2\times2)$ model. The alternative buckling dimer gives more chance for the adatoms to diffuse along the dimer rows.

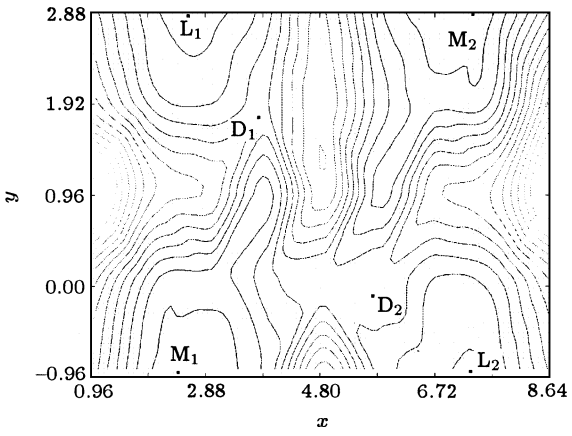


Fig.2. Contour plot of deposition energy difference of different Si adatom deposit positions on the $p(2\times2)$ Si(100) surface. The energy zero corresponds to the energetically lowest point. The spacing of the contour plots is 0.13eV and the letters and black dots denote the saddle points.

3.2. Growth on defective surface with SDV

The sample surface with a SDV is the easiest one for studying defective surfaces. An arbitrarily chosen dimer is simply removed from the perfect $p(2\times2)$ structure and then the system is fully relaxed via the ETB method with SD. Figure 3 shows the final equilibrium SDV structure. Compared with the equilibrium $p(2\times2)$ structure, the bond lengths of the dimers adjacent to the SDV are shortened by 0.002nm and the asymmetries of the dimers are enlarged by 0.005nm. The distance between one pair of atoms in the substrate layer across the SDV in Fig.3 becomes 0.026nm shorter, whereas that between the other pair becomes 0.063nm longer. So we can see that these four substrate atoms do not form any bonds. Compared with their coordinates, it can be observed clearly that atom B (C) is upward (downward). At the same time, atom D moves far away from the SDV and becomes deeper; atom E moves towards the SDV and becomes higher. The back bond (between C and E) is increased by 0.002nm, while other back bonds do not change much. The SDV causes an enlarged asymmetry that is also observed from the experiments;[1,23] and this agrees with other theoretical studies.[25,32] But in some of the results, the dimers adjacent to the SDV are pulled into the SDV slightly.[1,25] Our study shows that the total energy of the rebonding model (the four substrate atoms can rebond into two dimers) is 0.16eV higher. Jeong *et al*[32] also suggest that the nonbonding model is the most stable one. We attribute the observed closeness in experiments to the larger asymmetry or distortion of dimers. Due to the displacement of the atoms, the bond angles also become asymmetrical. The bond angles of the upper atom B are not equal with respect to the SDV. Toward the SDV, the bond angle is 88.1°; back to the SDV, it is 92.5°. The same situation happens to the down atom C, which has bond angles of 117.3° and 114.4° toward and back to the SDV, respectively.

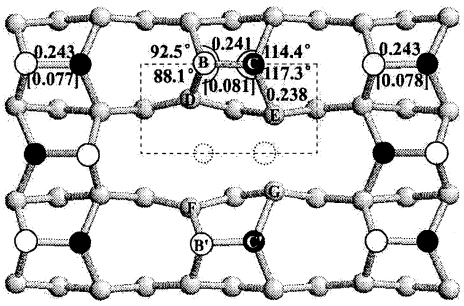


Fig.3. Top view of the fully relaxed $p(2\times2)$ Si(100) surface with a SDV. Dotted circles indicate the removed atoms.

On the deposition energy plot around SDV (Fig.4), the letters have the same meaning as those on the perfect surface. Because of the SDV, the diffusion path of an adatom around the SDV is more complex than that on the perfect surface. The diffusion paths($L_1 \rightarrow M$, $L_2 \rightarrow L_3$) are very smooth because the energy barrier is about 0.29–0.76eV. But the reversed diffusion paths have an energy barrier up to 1.89eV. On the middle of the dimer, the saddle point D_3, which in a perfect surface is a high point, will improve the possibility for the adatom to move into the SDV. One may think that adatoms will fill the SDV easily. But the situation is not so, because the activation energy is only about 0.53eV along the $D_1 \rightarrow D_2$ diffusion path. That is to say, the adatom can move into the SDV very easily and it can jump out of the SDV easily too. It would not move straightforwardly anyway. After it gets into the SDV, the adatom prefers to change the diffusion direction so that it can slip away from the SDV. STM studies show that adatoms cannot fill the SDV efficiently [30] and this is also obtained by Stillinger–Weber potential calculation.[25]

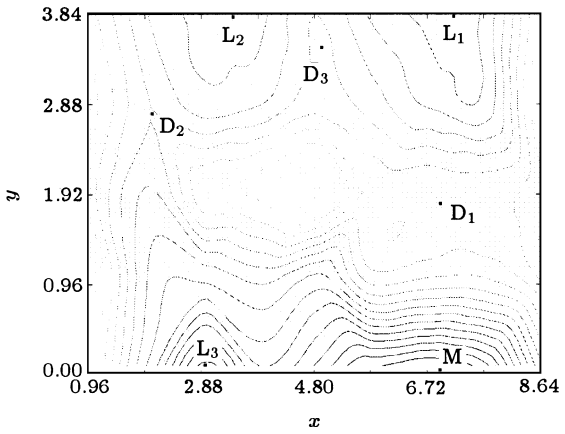


Fig.4. Contour plot of deposition energy difference of different Si adatom deposit positions around SDV on the $p(2\times2)$ Si(100) surface. The spacing of the contour plots is 0.15eV.

3.3. Growth on defective surface with double-dimer vacancy (DDV)

Experiments show that DDV defects are more popular than SDV. Two types of DDV are investigated. In A-type DDV (A-DDV, Fig.5(a)), the two missing dimers are aligned in the same row, and if the two missing dimers are aligned in the same line along the dimerization direction, that is, perpendicular to the dimer row, it is termed B-type DDV (B-DDV, Fig.5(b)).

After two adjacent dimers in the same row are removed from the $p(2\times2)$ model, the model is fully relaxed to obtain an energy minimal structure. Similar to the situation of the surface with a SDV, the asymmetries of the dimers and the substrate atoms are stronger than that of the perfect $p(2\times2)$ structure.

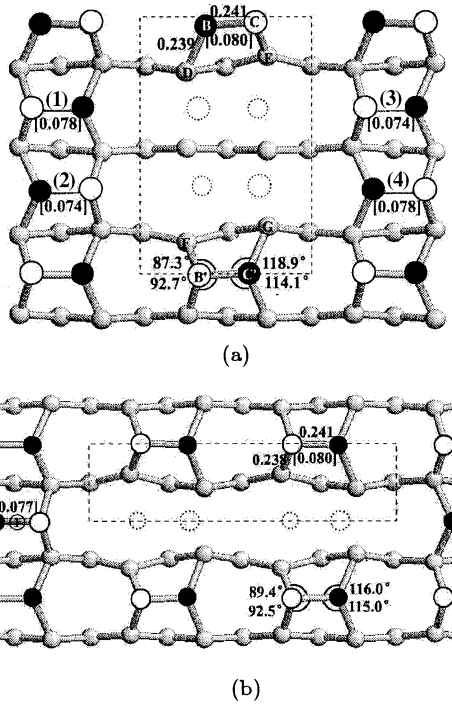


Fig.5. Top view of the fully relaxed $p(2\times2)$ Si(100) surface with (a)A-DDV (b)B-DDV.

Defects also influence the buckling of dimers not in the same row but in adjacent rows. In the SDV (the removed dimer also contains a higher atom and a lower atom), the asymmetry of the dimer close to the missing higher atom is increased by 0.002nm, while close to the missing lower atom, the asymmetry does not change much. In the DDV, this becomes clearer. On the left side of the row where A-DDV exists, just adjacent to the missing dimers, the asymmetry of dimer (1) is increased by 0.002nm because of the missing higher atom, while that of dimer (2) is decreased by 0.002nm because of the missing lower atom. On the right side, because dimer (3) is near the missing lower atom, the asymmetry of it is decreased by 0.002nm. Also, nearby the missing higher atom, dimer (4) has an enlarged asymmetry about 0.002nm. If it is B-DDV, the asymmetry of the dimer (1) ((2)) is increased by 0.001 (0.002)nm. Although the back bonds are about 0.239nm, the bond angles show larger asymmetries. The bond angle that face (back) to the vacancy is named the 'front (back) bond angle'. The front and back bond angles are equal on the perfect surface, but they are different on the defective surface. On the

SDV surface, for the higher dimer atom B, the difference between the front and back bond angles is 4.4°; for the atom C, it is 2.9°. On the A-DDV surface, the differences are 5.4° and 3.8° respectively, larger than those on SDV. But on the B-DDV surface, the differences (3.1° and 1.0° respectively) are slightly smaller than those on SDV. These asymmetries or distortions of dimers cause the closeness of the dimers neighbouring to the DVs.

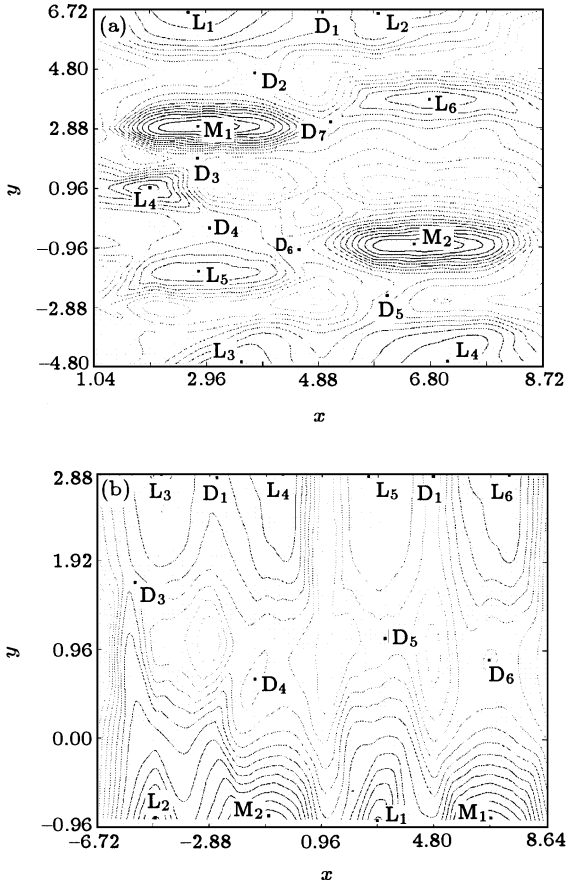


Fig.6. Contour plot of deposition energy difference of different Si adatom deposit positions around DDV on the $p(2\times2)$ Si(100) surface with (a)A-DDV (b)B-DDV. The spacing of the contour plots is 0.16eV (a) and 0.18eV (b).

Inspecting the deposition energy around A-DDV (Fig.6(a)) carefully, we find that the local minimum point beside the dimer and the saddle point on the dimer also increase chances for the adatom to fill into the A-DDV. So the adatom moves along the path $L_1 \rightarrow D_2 \rightarrow M_1$ with the energy barrier 0.80eV. If it goes straight, the energy barrier it should overcome is 1.68eV along the path $M_1 \rightarrow D_3 \rightarrow L_4$ or 1.47eV for the reversed path, while along the path $M_1 \rightarrow D_7 \rightarrow L_6$ the energy barrier confronted is only 0.96eV. So the adatom prefers to change the diffusion direction and moves out of the vacancy easily.

The situation of the deposition energy around B-DDV (Fig.6(b)) is a little like that on the surface with SDV. If the adatom overcomes an energy barrier about 0.75eV ($L_6 \rightarrow D_6 \rightarrow M_1$) or 0.41eV ($L_5 \rightarrow D_5 \rightarrow L_1$) and fills into the vacancy, it would overcome an energy barrier of 0.82eV to move out of the vacancy along $D_6 \rightarrow D_5 \rightarrow D_4 \rightarrow D_3$ or 1.20eV along $M_1 \rightarrow L_1 \rightarrow M_2 \rightarrow L_2$ instead of moving straight or back again with a higher energy barrier about 1.93eV. The adatom should overcome a higher energy barrier to hop out of both A and B type DDVs than SDV.

4. Conclusion

In this paper we have calculated the deposition energy of different Si adatom deposit positions near the perfect and defective $p(2\times2)$ Si(100) surfaces via the ETB method. Both SDV and two types of DDV structures have been studied. Several binding positions and some possible diffusion paths of a Si adatom on different sample surfaces have been achieved. Diffusion on the perfect surface has large anisotropy, and this anisotropy will be decreased due to the DVs introduced. Although the adatom can move into the DV easily, it cannot fill into it efficiently since it can move out of the DV easily too. Furthermore, the adatom can move in or out of SDV more easily than DDV because of its smaller energy barriers.

Here, only the situation of single adatom diffusion on perfect and defective surfaces have been considered and calculated, in which the defective surface contains a SDV or a DDV. Our future work will focus on the more complex crystal growth process for many other factors which can make the deposition of adatom much different, such as the adatom affecting reciprocal and other formations of surface defects, e.g. islands, kinks, etc.

References

[1] Hamers R J, Tromp R M and Demuth J E 1986 *Phys. Rev.* B **34** 5343

[2] Wang J, Arias T A and Joannopoulos J D 1993 *Phys. Rev.* B **47** 10497

[3] Weakliem P C, Zhang Z and Metiu H 1995 *Surf. Sci.* **336** 303

[4] Zandvliet H J W, Louwsma H K, Hegeman P E and Poelsma B 1995 *Phys. Rev. Lett.* **75** 3890
[5] Ramstad A, Brocks G and Kelly P J 1995 *Phys. Rev.* B **51** 14504
[6] Tromp R M, Hamers R J and Demuth J E 1985 *Phys. Rev. Lett.* **55** 1303
[7] Wolkow R A 1992 *Phys. Rev. Lett.* **68** 2636
[8] Chadi D J 1979 *Phys. Rev. Lett.* **43** 43
[9] Northrup J E 1993 *Phys. Rev.* B **47** 10032
[10] Binning G, Rohrer H, Gerber C and Weibel E 1982 *Phys. Rev. Lett.* **49** 57
[11] Brocks G, Kelly P J and Car R 1991 *Phys. Rev. Lett.* **66** 1729
[12] Zhang Z, Wu F, Zandvliet H J W, Poelsema B, Metiu H and Lagally M G 1995 *Phys. Rev. Lett.* **74** 3644
[13] Smith A P, Wiggs J K, Jonsson H, Yan H, Corrales L R, Nachtigall P and Jordan K D 1995 *J. Chem. Phys.* **102** 1044
[14] Fu C C, Weissmann M and Saul A 2001 *Surf. Sci.* **481** 97
[15] Borovsky B, Krueger M and Ganz E 1997 *Phys. Rev. Lett.* **78** 4229
[16] Borovsky B, Krueger M and Ganz E 1999 *Phys. Rev.* B **59** 1598
[17] Tromp R M and Mankos M 1998 *Phys. Rev. Lett.* **81** 1050
[18] Brocks G and Kelly P J 1996 *Phys. Rev. Lett.* **76** 2362
[19] Goringe C M and Bowler D R 1997 *Phys. Rev.* B **56** R7073
[20] Lee G D, Wang C Z, Lu Z Y and Ho K M 1998 *Phys. Rev. Lett.* **81** 5872
[21] Lee G D, Wang C Z, Lu Z Y and Ho K M 1999 *Surf. Sci.* **426** L427
[22] Yamasaki T, Uda T and Terakura K 1996 *Phys. Rev. Lett.* **76** 2949
[23] Yokoyama T and Takayanagi K 1997 *Phys. Rev.* B **56** 10483
[24] Tochihara H, Amakusa T and Iwatsuki M 1994 *Phys. Rev.* B **50** 12262
[25] Zhang Z and Metiu H 1993 *Phys. Rev.* B **48** 8166
[26] Men F K, Smith A R, Chao K J, Zhang Z and Shih C K 1995 *Phys. Rev.* B **52** R8650
[27] Fu C C, Weissmann M and Saul A 2001 *Surf. Sci.* **494** 119
[28] Okamoto M, Yokoyama T and Takayanagi K 1998 *Surf. Sci.* **402** 851
[29] Jin J M, Lewis L J, Milman V, Stich I and Payne M C 1993 *Phys. Rev.* B **48** 11465
[30] Mo Y W, Kleiner J, Webb M B and Lagally M G 1991 *Phys. Rev. Lett.* **66** 1998
[31] Alerhand O L and Mele E J 1987 *Phys. Rev.* B **35** 5533
[32] Jeong M S, Lee Y H and Hwang Y G 1995 *Phys. Rev.* B **51** 17151
[33] Lee S M and Lee Y H 1996 *Surf. Sci.* **347** 329
[34] Goodwin L, Skinner A J and Pettifor D G 1989 *Europhys. Lett.* **9** 701
[35] Fa W and Luo C L 2000 *Acta Phys. Sin.* **49** 430 (in Chinese)
[36] Li Y L and Luo C L 2002 *Acta Phys. Sin.* **51** 2589 (in Chinese)
[37] Hwang G S 2000 *Surf. Sci.* **4652** L789
[38] Mo Y W and Lagally M G 1991 *Surf. Sci.* **248** 313
[39] Lu Y T, Zhang Z and Metiu H 1991 *Surf. Sci.* **257** 19